Biochimica et Biophysica Acta 1828 (2013) 1066–1074

Contents lists available at SciVerse ScienceDirect

Biochimica et Biophysica Acta

journal homepage: www.elsevier.com/locate/bbamem

Structural and functional studies on a proline-rich peptide isolated from swine saliva endowed with antifungal activity towards *Cryptococcus neoformans*

Stefania Conti [a], Giorgia Radicioni [b], Tecla Ciociola [a], Renato Longhi [c], Luciano Polonelli [a], Rita Gatti [d], Tiziana Cabras [e], Irene Messana [e], Massimo Castagnola [b], Alberto Vitali [f,*]

[a] *Dipartimento di Scienze Biomediche, Biotecnologiche e Traslazionali, Unità di Microbiologia e Virologia, University of Parma, via Volturno 39, 43126, Parma, Italy*
[b] *Istituto di Biochimica e Biochimica Clinica, Faculty of Medicine, Catholic University, L.go F. Vito 1, 00168 Rome, Italy*
[c] *Istituto di Chimica per il Riconoscimento Molecolare, Italian National Research Council (CNR), via Mario Bianco 9, Milan, Italy*
[d] *Dipartimento di Scienze Biomediche, Biotecnologiche e Traslazionali, Unità di Anatomia, Istologia ed Embriologia, University of Parma, via Volturno 39, 43126, Parma, Italy*
[e] *Dipartimento di Scienze della Vita e dell'Ambiente, University of Cagliari, Cittadella Universitaria, Monserrato, 09042, Cagliari, Italy*
[f] *Istituto di Chimica per il Riconoscimento Molecolare, Italian National Research Council (CNR), Rome, L.go F. Vito,1 00168 Rome, Italy*

ARTICLE INFO

Article history:
Received 5 June 2012
Received in revised form 11 December 2012
Accepted 14 December 2012
Available online 26 December 2012

Keywords:
Proline-rich peptide
Antifungal
Circular dichroism
Membrane integrity
Polyproline-II
Cryptococcus neoformans

ABSTRACT

A proline-rich peptide of 2733 Da, isolated from pig parotid granule preparations was tested against different pathogenic fungi. It showed interesting antifungal activity towards a clinical isolate of *Cryptococcus neoformans*, with an EC_{50} of 2.2 μM. Neither cytotoxic nor haemolytic effects were observed towards mammalian cells. Circular dichroism and infrared spectroscopic studies showed that the peptide adopted a combination of polyproline type-II, β-turn and unordered conformations at physiological temperatures. Temperature dependent experiments evidenced a tendency to adopt a polyproline-II helix conformation. From experiments with lipid vesicles, Neutral Red Uptake (NRU), haemolytic assays, and confocal microscopy studies, it could be hypothesized that the peptide may exert its antifungal effect by interacting with an intracellular target rather than through membrane damage.

1. Introduction

Cryptococcosis is a serious and potentially life-threatening disease caused by environmental yeasts belonging to the genus *Cryptococcus*. Only *Cryptococcus neoformans* together with *C. gattii* are considered, among the many recognized species in the genus, the principal pathogens in humans. Previously, *C. neoformans* was defined as having two varieties — var. *neoformans* and var. *gattii*. They differed on the basis of antigenic specificity of the capsular polysaccharide: serotypes A, D and AD were recognized in var. *neoformans*, and serotypes B and C in var. *gattii*. Serotype A strains have been afterwards named *C. neoformans* var. *grubii* [1]. However, based on the elucidation of the genomic sequences, *C. gattii* is now considered a distinct species. Infection begins in the lung, following inhalation of environmental yeast cells. Initial manifestations depend likely on the fungal burden and the immune status of the host, and pulmonary cryptococcosis varies from a benign upper respiratory tract infection to a very severe bilateral pneumonia. The infection can spread through hematogenous dissemination. Cryptococci have a predilection to invade the central nervous system and can cause a life-threatening meningoencephalitis with involvement of motor and cognitive functions. Although cryptococcosis is mainly observed in cases of immune deficiency, many reports highlight its occurrence in patients without recognizable immune defects, indicating that the yeast can set up virulence mechanisms that provoke disease even in healthy individuals [2,3]. HIV-infected individuals are particularly prone to cryptococcal infection; cryptococcosis is an AIDS-defining illness and a major cause of mortality, particularly in sub-Saharan Africa [4]. The treatment regimens for cryptococcal meningitis are focused on amphotericin B, alone or in combination with flucytosine, for initial or induction treatment. Azoles, as fluconazole or itraconazole, remain the agents of choice for long-term maintenance therapy, to prevent relapses or as available therapeutic alternative. As for many other infectious diseases, treatment failures may occur because of antifungal drug resistance [5,6], so the development of new drugs with different mechanisms of action, including peptides endowed with antifungal activity [7,8], has to be pursued in order to face more threatening fungal infections in the future.

In this view, over the past decades a great interest has focused on antimicrobial peptides (AMPs) [9,10]. AMPs are a large and heterogeneous

Abbreviations: SPPS, (Solid Phase Peptide Synthesis); MALDI-TOF, (Matrix Assisted Laser Desorption Ionization – Time of flight); CD, (Circular Dichroism); ATR/FT-IR, (Attenuated Total Reflectance/Fourier Transform-Infra Red); PDA, (Polydiacetylene)

* Corresponding author at: ICRM-C.N.R. c/o Istituto di Biochimica e Biochimica Clinica, L.go F. Vito,1 I-00168 Rome, Italy. Tel.: +39 06 30154215; fax: +39 06 3053598.
E-mail address: alberto.vitali@icrm.cnr.it (A. Vitali).

0005-2736/$ – see front matter © 2012 Elsevier B.V. All rights reserved.
http://dx.doi.org/10.1016/j.bbamem.2012.12.013

family of peptides widespread in plant and animal kingdoms as important effectors of innate immunity. They have several common features, including the presence of a basic character with a positive net charge at physiological pH. AMPs are divided into sub-families depending on secondary structural similarities: the alpha-helical conformation is a common motif in the secondary structure of melittin, magainin, and the cathelicidin LL-37 [11]; beta strands with one or more disulfide bonds are common in defensins, cystatins, hepcidins, and thionins [12–15], while apidaecins, indolicidins, and histatins share a linear structure and are also characterized by the presence of specific amino-acids (e.g. Arg, Pro, His) [16,17]. Penaeidins, isolated from crustaceans, exhibit a peculiar structure being constituted by two distinct domains: a linear proline-rich and a cysteine rich one [18]. AMPs show antibacterial, antiviral and antifungal activities at a concentration ranging from nano to micromolar, and some of them are under development as new promising drugs [19]. Of particular interest is the fact that each class may exert killing activity through mechanisms of action different with respect to conventional antimicrobial drugs. Depending on experimental conditions, these mechanisms may be included in two main schemes: a) microbe cell membrane perturbation or disruption; b) interaction with intracellular targets [20].

A peculiar class of AMPs is represented by proline-rich peptides. They are small linear peptides characterized by a high content (up to 50%) of proline residues [21]. The most well known representative members of this class are the mammalian cathelicidins Bac-5, Bac-7 and PR-39 [22–24], crustacean penaeidins and insect apidaecins, but peptides derived from gastropods and earthworms were also described [25,26].

Due to their structural arrangement, the modalities by which proline-rich peptides exert their antimicrobial activity reside in the ability to translocate across the target organism membrane and interact with intracellular targets [27]. These are represented by DNA, enzymes, or protein complexes. In the latter case, peptides can interact with Proline-Rich Sequence Recognition Domains, such as Src Homology 3 (SH3) domains, being able to modulate different cellular mechanisms and pathways [28–30]. Proline-rich peptides are present in different body compartments and fluids in mammals, and saliva is one of the richest sources of these peptides in the mammalian order. Proteomic investigation of the pig saliva revealed the presence of interesting proline-rich peptides among which the main component, named SP-B peptide, showed to possess antifungal activity [31]. The aim of this study was to investigate the biological activities against pathogenic fungi of another minor component identified in swine saliva [32] and recently patented as anti-viral agent [pat. n° PCT/IB2012/050419].

2. Materials and methods

2.1. Peptide synthesis

SP-E peptide was assembled on an Applied Biosystem Peptide Synthesizer 433A (Foster City, CA, USA) on a preloaded proline-2-chlorotrityl resin (Novabiochem, Laufelfingen, CH) following the Fmoc-(N^{α}-9-Fluorenylmethyloxycarbonyl) protocol for stepwise solid phase peptide synthesis [33,34]. Fmoc-amino acids were from Novabiochem.

All couplings were carried out with 5 fold excess of activated amino acid in the presence of 10 equivalents of *N*-ethyldiisopropyl amine, using *N*-[(dimethylamino)-1-*H*-1,2,3-triazole-[4,5-β]pyridine-1-ylmethylene]-*N*-methylmethanaminium hexafluorophosphate *N*-oxide (HATU, PE Biosystems, Inc., Warrington, UK) as activating agent for the carboxy group. The fluoresceinated peptide was obtained by extending the N-termini of an aliquot (15%) of the assembled peptide-resin, with 8-(9-Fluorenyloxycarbonyl-amino)-3,6-dioxaoctanoic acid, removal of the Fmoc protecting group and coupling of 5-Carboxyfluorescein (FAM), mediated with 1-Hydroxybenzotriazole and *N*, *N*′-Diisopropylcarbodiimide. The fluoresceinated peptide was released from the resin and purified by the same procedures adopted for the free-peptide. At the end of peptide chain assembly, the peptide was cleaved from the resin by treatment with a mixture of 80% trifluoroacetic acid, 5% water, 5% phenol, 5% thioanisole, 2.5% ethandithiol and 2.5% triisopropylsilane for 3 h at room temperature, with concomitant side chain deprotection. The resin was filtered and the peptide was precipitated in cold *tert*-butylmethyl ether. After centrifugation and washing with *tert*-butylmethyl ether the peptide was suspended in 5% aqueous acetic acid and freeze-dried. Analytical and semipreparative Reversed Phase High Performance Liquid Chromatography (RP-HPLC) was carried out on a Tri Rotar-VI HPLC system equipped with a MD-910 multichannel detector for analytical purposes or with a Uvidec-100-VI variable UV detector for preparative purposes (all from JASCO, Tokyo, Japan). Analytical RP-HPLC was performed on a Jupiter 5 μ C18 300 Å column (150×4.6 mm, Phenomenex, Torrance, CA, USA). Semipreparative RP-HPLC was performed on a Jupiter 10 μ C18 300 Å column (250×21.2 mm, Phenomenex). Linear gradients of acetonitrile in aqueous 0.1% TFA (v/v) were used to elute bound peptide. MALDI-TOF mass spectrometry analysis was performed on a Autoflex workstation (Bruker Daltonics, Bremen, DE). Observed experimental values for peptide masses were in agreement with theoretical calculated values.

2.2. CD and ATR/FT-IR measurements

CD spectra were obtained on a Jasco J-600 spectrophotometer equipped with a thermostatic temperature controller. CD spectra were recorded in quartz cell of 0.1 cm path length at 25 °C between 190 and 250 nm, using a 2.0 nm bandwidth and a scanning rate of 20 nm/min with a wavelength step of 0.1 nm and a time constant of 0.1 s. SP-E peptide was dissolved in 10 mM sodium phosphate buffer at pH 7.4. A TFE 30% (v/v) aqueous solution was also employed. CD band intensities are expressed as molar ellipticities, ($[\theta]_M$ in deg cm^2 $dmol^{-1}\times10^{-3}$).

ATR/FT-IR spectra were recorded on a Spectrum One (Perkin–Elmer) spectrophotometer equipped with an ATR accessory with a ZnSe reflection element. Prior to analysis, SP-E synthetic peptide was dissolved in 20 mM HCl and subsequently freeze-dried twice in order to remove the residual TFA derived from peptide purification. Spectra were recorded after 40 scans at a 1 cm^{-1} of resolution. The samples were dissolved in 10 mM sodium phosphate buffer, pH 7.4. An open beam background spectrum of clean crystal was recorded. Subsequently the buffer solution spectrum was recorded followed by the peptide spectrum measurement. The spectra of buffers alone were hence subtracted from the peptide ones. During measurements performed at 25 °C, the crystal was continually flushed with nitrogen to eliminate residual water vapors. Usually 1 μL of a 1 mg/mL (w/v) solution of SP-E peptide was employed for any measurement.

2.3. Spectroscopic data treatment

ATR FT/IR spectra were used to obtain second derivative spectra with Peak Fit 4.12 software (Sea Solve Software, Inc., San Jose, CA, USA). A 20% smoothing process, employing the Savitzky-Golay algorithm, was performed and the resulting peaks were used as a reference for the subsequent peak fitting analysis performed with the same program. A linear baseline was employed and Gaussian peaks were produced after an iterative adjustment of data until the SSE statistical parameter was under 1×10^{-4}, indicating a good fitting analysis. The resulting peak areas of Amide I were used to determine the contribution of each secondary structure motif.

Circular dichroism spectra were analyzed employing Selcon3 program available on Dichroweb web site (http://dichroweb.cryst.bbk.ac.uk/html/home.shtml) [35]. The data were inserted as requested by the web site manager in the range between 190 and 250 nm. The obtained results satisfied the three basic selection rules: sum of

secondary structure fractions was >1, each fraction was >0.025, the RMS deviation between the reconstructed and experimental CD was <0.25 Δε, according to software recommendation.

2.4. In vitro evaluation of fungicidal activity

The fungicidal activity *in vitro* was assessed by colony forming unit (CFU) assays as previously described [31,36]. Fungi to be tested (*Candida albicans* UP10, *C. neoformans* AIDS 25, and *Aspergillus fumigatus* UP1) were grown in Sabouraud dextrose agar plates at 30 °C for 24–48 h (yeasts) or 4–5 days (*A. fumigatus*). Yeast cells and conidia were suspended in sterile distilled water ($3–5\times10^4$ cells/mL) and 10 μL of suspensions were added to 90 μL of H_2O containing the synthetic peptide at different concentrations (36.5 μM to 1.1 μM). H_2O alone served as a control. After incubation for 6 h (yeasts) or 18 h (*A. fumigatus*) at 37 °C with the respective reagents, the fungal cells were dispensed and streaked on the surface of Sabouraud agar plates. After incubation for 48–72 h at 30 °C, colonies were enumerated. Each experiment was performed in triplicate. Peptide fungicidal activity was determined as the percentage of CFU inhibition, according to the formula $100-(\text{CFU experimental group/CFU control})\times100$. Peptide half maximal effective concentration (EC_{50}), was calculated by nonlinear regression analysis using Graph Pad Prism 4.01 software. In preliminary experiments, the previously described proline-rich peptide SP-B, endowed with antifungal activity [31], was used as a positive control.

2.5. Cells and treatments

Mouse 3T3-fibroblasts (Swiss albino mouse cell line) (Istituto Zooprofilattico, Brescia, Italy) and HL-60 cells were grown in a 5% CO_2 atmosphere at 37 °C in DMEM (Dulbecco's Modified Eagle Medium) with Hepes (10 mM), glucose (1.0 g/L), $NaHCO_3$ (3.7 g/L), penicillin (100 units/mL), streptomycin (100 μg/mL) and 10% FCS (fetal calf serum). Human oral squamous carcinoma keratinocytes (PE/CA PJ15, ECACC, UK), were grown in the above reported conditions, but employing IDMEM as basal medium.

2.6. Cytotoxicity tests

The possible cytotoxic effects of the SP-E peptide were studied on 3T3-Swiss, HL-60 and PE/CA PJ15 cell lines using Neutral Red Uptake (NRU) and thiazolyl blue tetrazolium bromide (MTT) tests. In order to evaluate the cytotoxic effects of SP-E, the freeze-dried peptide was prepared at different final concentrations (2.5, 5, 10, 20 and 50 μM) dissolved in basal medium (2.2 mL) checking for final pH. Cells (1×10^4) in basal medium (200 μL) were seeded in individual wells of a 96-well tissue culture plate and cultured to sub-confluent monolayer for 24 h. Cellular viability was evaluated by NRU and MTT tests, after 24 h, 48 h, and 72 h after addition of the peptide at 37 °C at different concentrations (2.5, 5, 10, 20 and 50 μM). NRU assay was performed according to Borenfreund [37]: a Neutral Red aqueous solution (0.4 %) was added to each well to obtain a final concentration of 50 μg/mL and, after incubation for 4 h at 37 °C, the supernatant was discharged. The intracellular Neutral Red was revealed by adding a solution of 50% ethanol with 1% acetic acid (200 μL). The optical density (OD) of the solution was determined using an automatic microplate photometer (Packard Spectracount™, Packard BioScience Company, Meriden, CT, USA) at a wavelength of 540 nm. MTT test was performed according to Wataha et al. [38]: 20 μL of a 5 mg/mL solution of MTT in PBS were added to the medium (200 μL) and, after incubation for 4 h at 37 °C, the intracellular formazan crystals produced were solubilized with a solution of HCl in isopropanol (4×10^{-2} M, 200 μL). Absorbance was measured at 570 nm. Each experiment was performed in sextuplicate and the cell cytotoxicity was calculated according to Hashieh et al. [39].

2.7. PDA-phospholipid colorimetric vesicle assay

Dimiristoyl-phosphatidyl glicerol (DMPG), phosphatidylcholine (PC) and 10,12-Tricosadiynoic acid (polydiacetylene, PDA), were all purchased from Sigma-Aldrich (St. Louis, MO, USA). Phospholipid vesicles were prepared as described in [40] with slight modifications. Briefly, DMPG and PC were combined with PDA in a 2:1:2 DMPG/PC/PDA ratio obtaining a final concentration of total lipids of 1 mM. After solubilization in a chloroform:methanol 2:1 solution and drying under rotary evaporation, the mixtures were resuspended in ultrapure water, warmed at 70 °C and sonicated. The resulting opalescent solution was cooled at 4 °C overnight. Before each experiment the vesicle preparations were centrifuged at 2000 rpm for 15 minutes at 25 °C and the suspension used for subsequent polymerization achieved using UV irradiation at 220 nm for a few seconds. The resulting mixtures exhibited an intense blue colour. The experiments were performed with a spectrophotometer (Agilent 8453, Santa Clara, CA, USA) following the signals at 500 and 640 nm in the time. In order to quantitatively evaluate the colorimetric response the extent of blue-to-red color transition was calculated by the colorimetric response (%CR), which is defined as

$$\%CR = [(PB_0 - PB_1)/PB_0] \times 100$$

where $PB = A_{640}/(A_{640}+A_{500})$, A is the absorbance either at 640 nm (blue colour) or at 500 nm (red component) in the UV-vis spectrum, PB_0 is the red/blue ratio of the control sample (before induction of color change), and PB_I is the value obtained for the vesicle solution after addition of peptides. Melittin, an antimicrobial peptide characterized by an alpha helical conformation and known for its pore forming activity, was employed as a positive control [41].

2.8. Haemolytic and stability assays

Haemolytic activity was tested on human erythrocytes (group 0 Rh+) (RBCs) collected from a healthy donor in tubes containing heparin (20 U/ml). RBCs were harvested by centrifugation for 12 min at 2000 g (room temperature), washed twice with PBS (9 mM sodium phosphate, pH 7.4, 150 mM NaCl), and resuspended in PBS. Serial dilutions of SP-E peptide in PBS were then prepared and added to the RBC solution to a final concentration of 25, 125, and 250 μM in the volume of 200 μl (final erythrocyte concentration, 2.5% v/v), the same concentration was in triplicate. After 1 h of incubation at 37 °C the plates were centrifuged for 5 min at 1500 g. The supernatants were hence transferred in a microplate and release of hemoglobin was monitored by measuring the absorbance at 540 nm. Controls for zero hemolysis (blank) and 100% hemolysis consisted of RBCs suspended in PBS and Triton X-100 0.5%, respectively. Melittin at a concentration of 5 μM served as a further positive control.

Stability assays were performed incubating SP-E peptide for 48 h in human serum. At intervals, aliquots of the mixture were taken and centrifuged for 3 min at 12,000 rpm. The supernatant was mixed with 0,2% aqueous TFA and injected in a RP–HPLC–ESI–MS apparatus (Surveyor HPLC system – ThermoFisher, San Jose, CA, USA) connected by a T splitter to a photodiode array detector and to a LCQ Deca XP Plus mass spectrometer (ThermoFisher). The chromatographic column was a Vydac (Hesperia, CA, USA) C8 with 5 μm particle diameter (column dimensions 150 mm × 2.1 mm). The following solutions were utilized: (eluent A) 0.056% (v/v) aqueous TFA and (eluent B) 0.05% (v/v) TFA in acetonitrile:water 80/20. Peptide was eluted using a linear gradient from 0 to 55% of B for 40 min, at a flow rate of 0.30 mL/min. The T splitter permitted 0.20 mL/min to flow toward the diode array detector and 0.10 mL/min to flow toward the ESI source. Mass spectra were collected every 3 ms in the positive

ion mode. The MS spray voltage was 4.50 kV, and the capillary temperature was 220 °C.

2.9. Confocal microscopy studies

Interaction between yeast cells and 5-carboxyfluorescein (FAM)-labelled SP-E was followed in time lapse with confocal microscopy (LSM 510 Meta scan head integrated with the Axiovert 200 M inverted microscope, Carl Zeiss, Jena, Germany). Analysis was performed on living *C. neoformans* AIDS 25 cells seeded on coverslips mounted in a special flow chamber [42] and placed in a commercially available incubation system (Kit Cell Observer, Carl Zeiss). A selected field was kept and observed along the time lapse experiment. Images were taken every 15 min up to 3 h. At the beginning propidium iodide (PI) (Invitrogen, Milan, Italy), a non-vital nuclear stain commonly used for identifying dead cells, was used (22 μM). After 20 min, FAM-peptide was added (final concentration 60 μg/mL).

Samples were observed through a 63 × NA 1.4 plan apo oil objective. PI and FAM were excited with 543 nm He-Ne and 488 nm argon laser lines, respectively. Acquisition was carried out in a multitrack mode (namely through consecutive and independent optical pathways).

3. Results and discussion

In a previous study a series of proline-rich peptides were isolated from secretory granules of pig parotid glands and characterized by means of LC-MS-MS and Edman degradation [32]. Among them, a peptide named SP-E (2733 Da, sequence: NH_2-DKPKKKPPPPAGPPPPPPPPPGPPPPGP-28, F1SQ50-UniProtKB/TrEMBL) resulted to be the most promising from a preliminary antimicrobial screening. The same peptide has been recently patented as an anti-viral agent [PCT/IB2012/050419]. Due to the low amount obtainable from parotid granules extracts (nanomolar range [32]) a synthetic form of SP-E was produced and used for all the experimental purposes. The synthesis of SP-E was almost easily achieved, due to the presence of the non hindered amino acids glycine and proline: 3 glycine residues and 19 proline residues over 28 residues. After assembly via SPPS, the peptide was recovered in high yield and homogeneously from the resin. The final peptide purification, carried out by RP-HPLC, gave rise to a high-purity preparation as assessed by MALDI-TOF mass spectrometry analysis (Fig. 1).

3.1. Structural studies

Porcine peptide SP-E was studied by means of CD and FTIR spectroscopy. SP-E shows structural peculiar features such as a polar head conferring to the peptide a highly basic character (theoretical pI = 10.0), followed by a non polar tail in which a nonamer of prolines is found. The far UV-CD spectrum of SP-E in 10 mM phosphate buffer at pH 7.4 and at 30 °C, showed a broad negative band around 202 nm and a slightly positive band at 222 nm (Fig. 2, top, curve b), resembling spectra of other proline-rich peptides in similar conditions [43]. In order to evidence the presence of "hidden" structures, different spectra were taken in the temperature range between 0 °C to 65 °C. At 65 °C, a decrease of the negative band was observed together with the disappearing of the weak positive band at 222 nm (Fig. 2, top, curve a). Conversely, by decreasing the temperature until 0 °C an increase of the negative band at 200 nm and an increase of the positive band at 220 nm were observed (Fig. 2, top, curve c). An isodichroic point was visible at 208 nm indicating an equilibrium among the intermediate structures during the thermal transitions. A typical profile of an *all trans* left handed polyproline II (PP-II) helix is characterized by a strong signal at 202 nm and by a positive band at 224 nm [44–47]. The fact that SP-E shows such a feature at low temperatures may indicate an intrinsic propensity to adopt this kind of secondary structure in favourable circumstances. This may be the case for example of an interaction with a ligand surface where the structural constraints, consequence of the binding, "freeze" the structure in a PP-II helix. Experiments performed in a 30% trifluorethanol solution at 30 °C did not evidence any conformational change (data not shown).

Consistently with the CD results, the FTIR-ATR spectrum of SP-E was characterized by two major bands: the Amide I centered at 1622 cm^{-1}, and a band at 1439 cm^{-1} (Fig. 2, bottom). The band at 1622 cm^{-1} could be ascribed to a PP-II helix [43] while the strong band at 1439 cm^{-1} was assigned to the proline side-chain signals [48]. The analysis of the Amide I (Table 1) gave as a result four main components: at 1627 cm^{-1} (38.9%), at 1644 cm^{-1} (22.7%), at 1613 cm^{-1} (30.6 %), and at 1661 cm^{-1} (7.67 %). These data indicate a conformational propensity of SP-E to adopt a mixture of PP-II, unordered and turn motifs.

The movements around the dihedral angles are very close between an unordered and a PP-II helix structure and hence may be

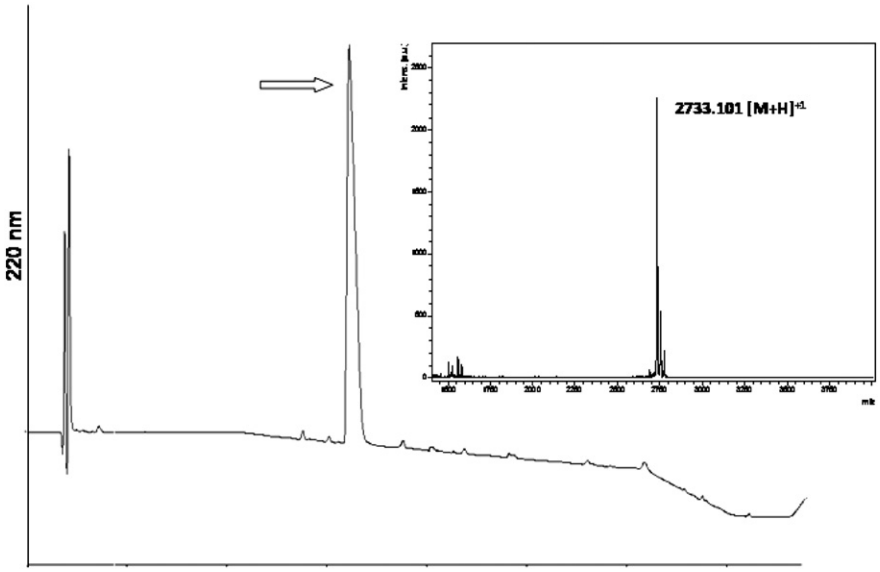

Fig. 1. RP-HPLC chromatogram related to SP-E peptide purification after SPPS synthesis. The chromatogram has been recorded at 220 nm. The arrow indicates the peak corresponding to SP-E. Inset: MALDI-TOF spectrum of collected peak indicating the purity of the preparation.

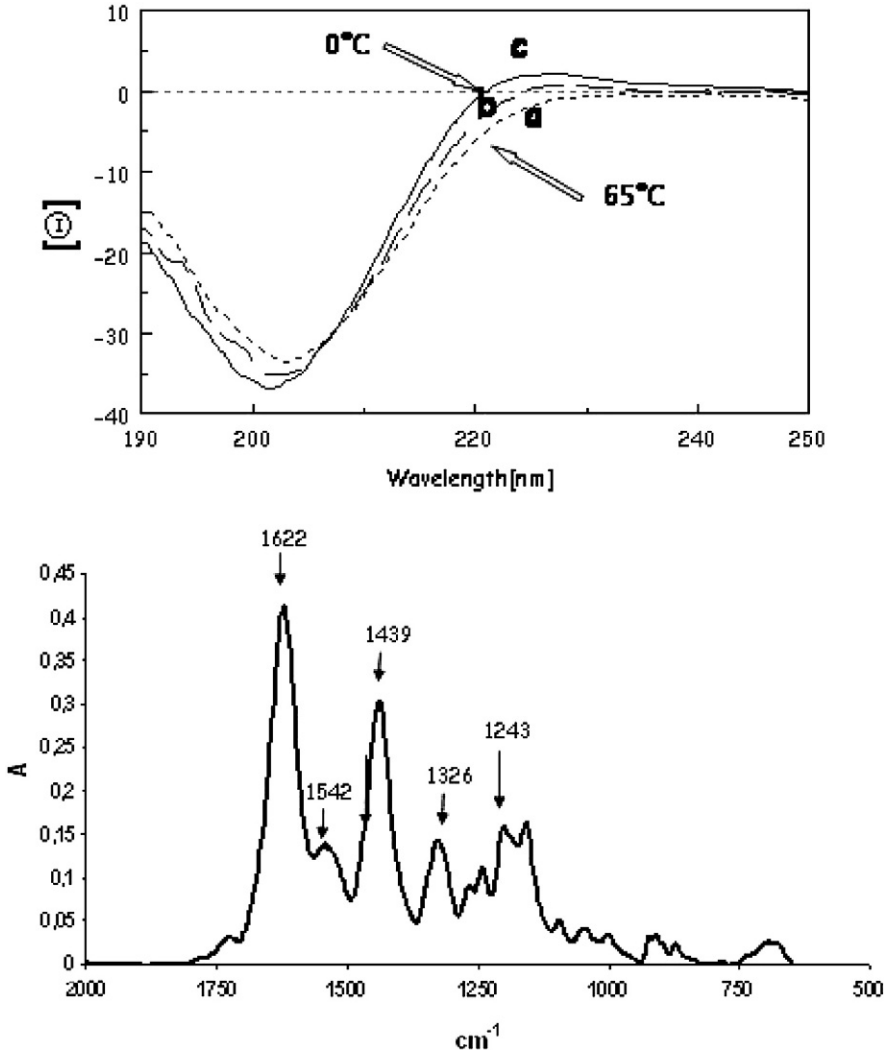

Fig. 2. Far UV-CD (top) and ATR/FT-IR (bottom) spectra of SP-E. (top) The peptide (10 μM) was dissolved in a 10 mM phosphate buffer at pH 7.4. The spectra were taken at different temperatures, for clarity in the scheme are shown only three curves: line a, 65 °C, line b 30 °C, and line c 0 °C. (bottom) The ATR/FT-IR spectrum was taken as reported in Materials and methods section. Arrows indicate the Amide I band centered at 1622 cm^{-1} attributable to a polyproline-II helix conformation and the peak at 1439 cm^{-1} ascribed to the proline residues.

temperature-modulated. Similarly the transition between unordered and turn motifs may also be easily driven by temperature. This overall view suggests for SP-E a flexible structure, consistently with recent descriptions of proline-rich peptides described as flexible structures covering different conformational landscapes, in contrast with the classical "rigid rod" vision [49].

Such a feature may be important for the expression of SP-E fungicidal activity, and the presence of proline stretches may be of relevance for potential interactions with Proline-Rich Sequence Recognition Domains [50]. If so, many metabolic points crucial for cell viability (e.g. cytoskeleton modelling, motility, transduction pathways etc.), may be targeted by the peptide which may act as a modulatory agent.

Table 1
Areas of residuals obtained after deconvolution of Amide-I band of SP-E. Deconvolution was performed with Peak-Fit software (see Materials and methods section for details).

Peak	Residuals area (%)	Centroid	Assignements
1	30.6	1613.1	β-turn
2	38.9	1627.2	Polyproline-II
3	22.7	1644.1	Unordered
4	7.67	1661.2	β-turn
Total	100.0		

3.2. Biological activity

The SP-E peptide was tested for antifungal activity against the clinical isolates *C. neoformans* AIDS 25, *A. fumigatus* UP1 and *C. albicans* UP10. The highest growth inhibition was obtained against *C. neoformans* (Scheme 1) with an EC_{50} value of 2.2 μM (95% confidence intervals 3.02–4.78). EC_{50} values towards *C. albicans* UP10 and *A. fumigatus* UP1 were 34.7 and 58.68 μM, respectively (95% confidence intervals 31.3–38.4 and 43.6–78.8). A negligible antibacterial activity was detected against *Pseudomonas aeruginosa* and *Staphylococcus aureus* strains, at concentrations above 100 μM, while SP-E proved to be active against *Salmonella typhimurium* and *Escherichia coli* at micromolar concentrations (data not shown). Future work will be devoted to the investigation of SP-E antibacterial activity. These preliminary results are consistent with previous reports on antibacterial activity of proline-rich peptides [27]. The short PRPs derived from insects and the longer mammalian relatives, such as PR-39, bactenecins and prophenins, are mostly active against Gram-negative bacteria [51]. Some of these peptides were also reported to exert antifungal activity; in particular a bactenecin-7 fragment proved to be significantly active against *C. neoformans* clinical isolates and collection strains [52], and bactenecin-5 fragments showed a candidacidal activity similar to that of the entire molecule [53]. The

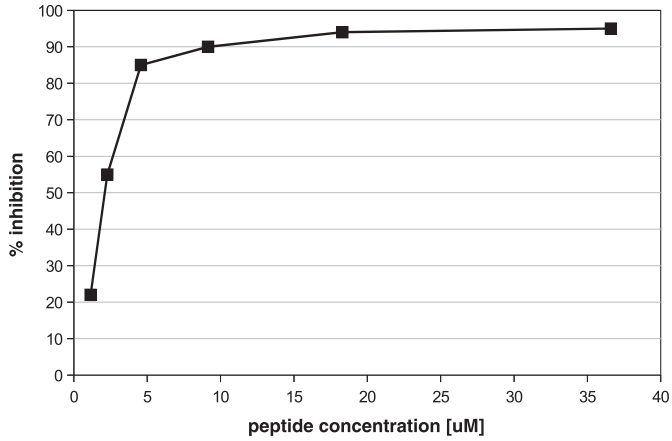

Scheme 1. *In vitro* fungicidal activity of SP-E peptide. The estimated EC_{50} for the activity of SP-E against *Cryptococcus neoformans* AIDS 25 was 2.2 μM.

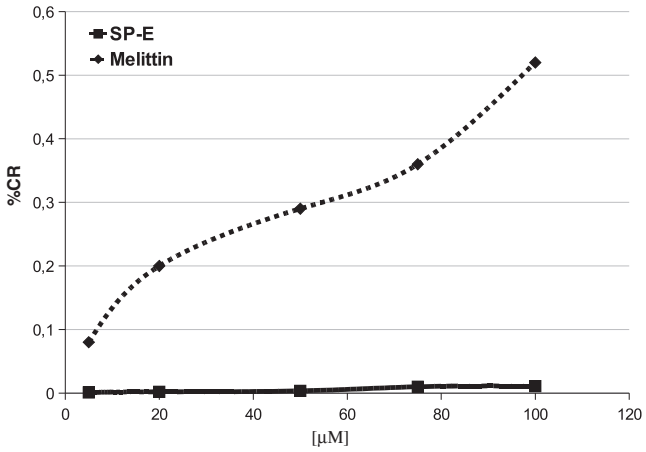

Scheme 2. Phospholipid/Polydiacetylene colorimetric vesicle assay. Colorimetric response (%CR) induced by different concentrations of melittin or SP-E peptide on PC/DMPG/PDA vesiscles at pH 7.4 was determined. % CR represents the percentage of colour transition from blue (integer vesicles) to pink–red (perturbed vesicles) spectrophotometrically monitored at 640 nm and 500 nm, respectively.

peculiar primary sequence of SP-E is almost new in the proline-rich peptides panorama. SP-E and Bac-5 share a PP-II conformational arrangement and a positive charge (in Bac-5 due to Arg residues); these two characteristics were in fact found to be essential for the exploitation of the antifungal activity in Bac-5. Moreover, Bac-5 and SP-E showed comparable antifungal activities in terms of fungal growth inhibition [53].

In order to examine possible modulatory, cytotoxic or pro-apoptotic effects, SP-E was tested on some mammalian cell lines. Cytotoxicity was evaluated on the murine 3T3 fibroblast cell line, HL60 monocytes and the oral squamous carcinoma cell line PECA/PJ15. In all the tests performed SP-E did not show particular toxicity even at concentration of 50 μM, as evidenced by MTT test (data not shown). NRU assay also indicated an absence of membrane damage deriving from an interaction with the peptide. Finally, the haemolytic activity was tested on human red blood cells. SP-E showed no hemolytic activity at the concentrations and time investigated, as demonstrated by the mean absorbance values of released hemoglobin (SP-E 25 μM, 0.024 ± 0.002; SP-E 125 μM, 0.021 ± 0.002; SP-E 250 μM, 0.026 ± 0.006) that did not differ from the ones of the negative control (PBS, 0.027 ± 0.002) in comparison to the positive control (Triton X-100 0.5%, 2.309 ± 0.012; melittin 5 μM, 2.122 ± 0.083).

3.3. Effects on phospholipid vesicles and confocal microscopy studies

The majority of the antimicrobial peptides exert their activity through a perturbation of the outer membrane with different mechanisms [54]. Several proline-rich peptides are also known to be able to translocate across the cell membranes behaving as cell-penetrating peptides (CPPs), indicating with this term the ability to enter the cell without damaging its outer membrane [55]. In order to investigate this aspect, we performed the test reported in [40]. Briefly, a vesicle preparation was obtained by sonicating a solution of polydiacetylene (PDA) and an appropriate phospholipid mixture (phosphatidylcholine or dimiristoyl phosphatidylglycerol, 1 mM total lipids) and then exposing it to UV light at 220 nm. Polymerization of PDA was assessed by the

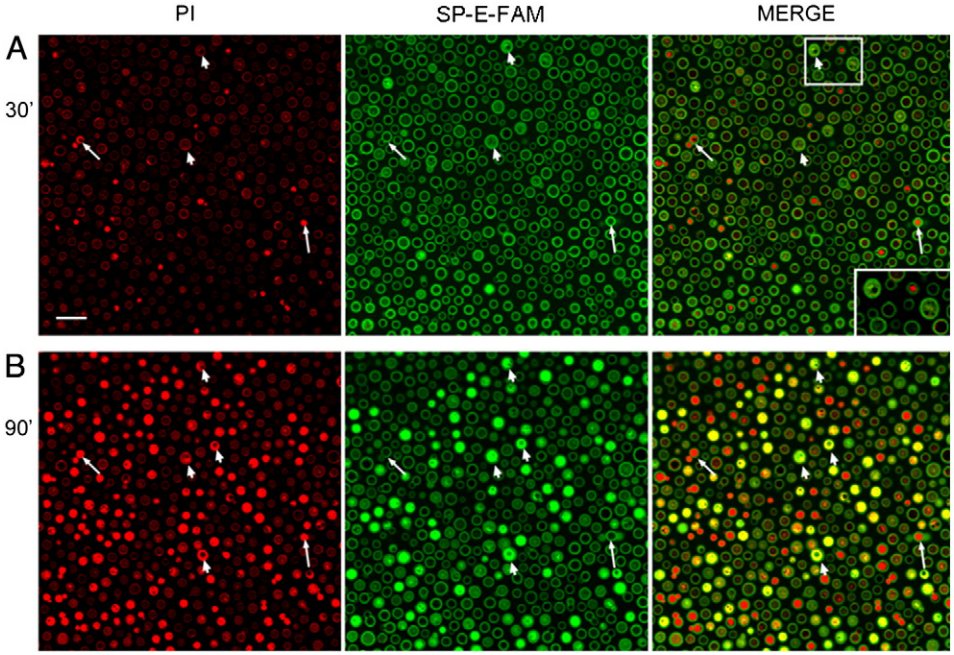

Fig. 3. Internalization of SP-E into *Cryptococcus neoformans* cells. Confocal images of living yeast cells incubated in the presence of FAM-labelled peptide (22 μM) for 30 min (A) and 90 min (B). The same field is shown. Bar = 20 μm. SP-E is efficiently internalized by yeast cells that, after 90 min of treatment are no longer viable (arrow heads). Non-viable yeast cells in the inoculum do not internalize SP-E (arrows). In the inset, one cell at larger magnification is shown to highlight the lack of peptide penetration in the cell vacuole.

transition to blue colour of the solution. Increasing amounts of peptide were mixed with the vesicles so obtained and the transition from blue (640 nm) to pinkish colour (500 nm) was monitored. The resulting conversion rates (CR) value gave the entity of the perturbation. Melittin, an antimicrobial peptide characterized by an alpha helical conformation and known for its pore forming activity, was employed as a positive control [41]. Melittin provoked a rapid conversion of the colour from blue to pink already at 5 μM (10% CR), whereas SP-E did not, even at higher concentrations (100 μM, Scheme 2), indicating an absence of perturbation of the lipid vesicles. These results are in fairly agreement with the data obtained from NRU tests, and suggest that the mechanism of action of SP-E is not based on the membrane perturbation, but more likely on the interaction with a target inside the cell [21].

To demonstrate SP-E penetration into yeast cells, confocal microscopy studies were performed with FAM-labelled peptide. Viable *C. neoformans* cells were treated with PI, and incubated for 3 h in the presence of SP-E-FAM. Confocal images were taken every 15 min. As shown in Fig. 3, panel A, after 30 min of incubation SP-E binds to the surface of all yeast cells, while internalization was seen in some of them. SP-E did not penetrate in non-viable yeast cells of the inoculum, suggesting an active process of internalization. After 90 min of treatment with SP-E (Fig. 3, panel B), internalization was seen in most of the cells, some of which were already killed, as shown by PI penetration.

3.4. Peptide stability experiments

In order to establish the stability of the peptide in a blood-like environment, SP-E peptide was incubated for 24 h in human serum. After 8 and 24 h aliquots of the solution were collected, precipitated with 0.1% TFA and analyzed by HPLC-ESI-MS. No proteolytic fragment

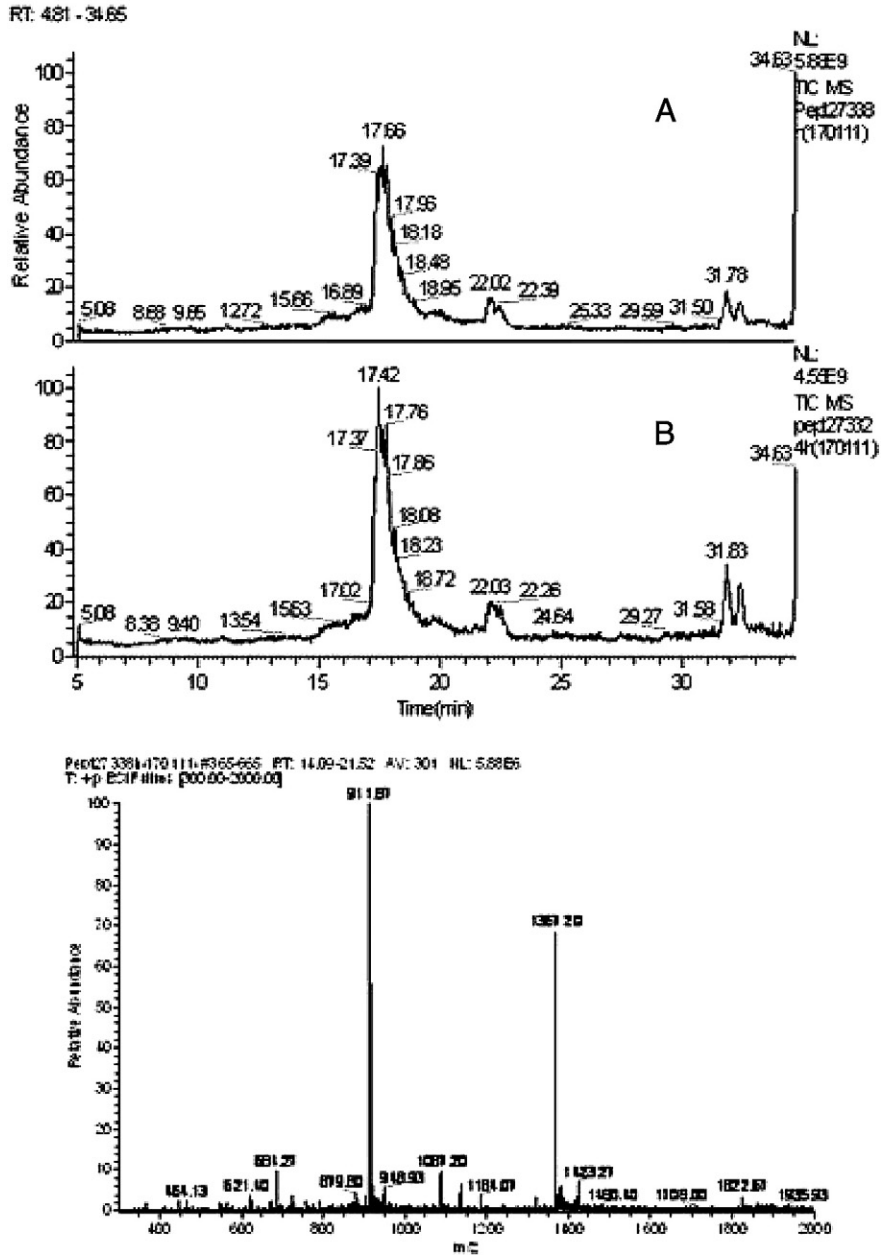

Fig. 4. Stability experiments of SP-E proline-rich peptide. A, TIC chromatogram showing peptide (17.66 min, R.T.) after 8 h of incubation in human serum; B, TIC chromatogram showing SP-E (17.42 min, R.T.) after 24 h of incubation in serum. The relative abundances are very similar indicating an overall stability of the peptide. In the third frame are reported the m/z values of the main peak, the $[M+2H]^{2+}$ (1367.20) and $[M+3H]^{3+}$ (911.87). Their deconvolution gives the value of 2733.55 amu.

could be detected neither at 8 h (Fig. 4, A), or after 24 h (Fig. 4, B). This result indicates a high degree of stability of the peptide, despite the high presence of lysine residues which may be targets for trypsin-like enzymes. Conversely, the presence of many proline residues may be at the basis of the resistence to proteolysis events.

4. Conclusions

SP-E peptide is an interesting member of proline-rich peptides family, showing an antifungal activity especially towards *C. neoformans*, in the EC_{50} micromolar range.

The absence of cytotoxic effects versus mammalian cells, even at concentrations well above those able to inhibit fungal growth, and the high degree of stability suggest that this peptide may be candidate as a promising antifungal agent. The lack of damage to cell membranes and phospholipid vesicles, together with the results of confocal microscopy studies suggest an intracellular target for this peptide.

Acknowledgements

We acknowledge the financial support of the Nando Peretti Foundation, Università di Cagliari, Università Cattolica in Rome, MIUR, Italian National Research Council (CNR), and Regione Sardegna, and thanks to their programs of scientific research promotion and diffusion.

References

[1] S.P. Franzot, I.F. Salkin, A. Casadevall, *Cryptococcus neoformans* var. *grubii*: separate varietal status for *Cryptococcus neoformans* serotype A isolates, J. Clin. Microbiol. 37 (1999) 838–840.
[2] J.W. Kronstad, R. Attarian, B. Cadieux, J. Choi, C.A. D'Souza, E.J. Griffiths, J.M. Geddes, G. Hu, W.H. Jung, M. Kretschmer, S. Saikia, J. Wang, Expanding fungal pathogenesis: *Cryptococcus* breaks out of the opportunistic box, Nat. Rev. Microbiol. 9 (2011) 193–203.
[3] M.A. Olszewski, Y. Zhang, G.B. Huffnagle, Mechanisms of cryptococcal virulence and persistence, Future Microbiol. 8 (2010) 1269–1288.
[4] B.J. Park, K.A. Wannemuehler, B.J. Marston, N. Govender, P.G. Pappas, T.M. Chiller, Estimation of the current global burden of cryptococcal meningitis among persons living with HIV/AIDS, AIDS 23 (2009) 525–530.
[5] J.R. Perfect, G.M. Cox, Drug resistance in *Cryptococcus neoformans*, Drug Resist. Updates 2 (1999) 259–269.
[6] E. Sionov, H. Lee, Y.C. Chang, K.J. Kwon-Chung, *Cryptococcus neoformans* overcomes stress of azole drugs by formation of disomy in specific multiple chromosomes, PLoS Pathog. 6 (2010) e1000848, http://dx.doi.org/10.1371/journal.ppat.1000848.
[7] E. Cenci, F. Bistoni, A. Mencacci, S. Perito, W. Magliani, S. Conti, L. Polonelli, A. Vecchiarelli, A synthetic peptide as a novel anticryptococcal agent, Cell. Microbiol. 6 (2004) 953–961.
[8] F. Barchiesi, A. Giacometti, O. Cirioni, D. Arzeni, C. Silvestri, W. Kamysz, A. Abbruzzetti, A. Riva, E. Kamysz, G. Scalise, In vitro activity of the synthetic lipopeptide PAL-Lys-Lys-NH_2 alone and in combination with antifungal agents against clinical isolates of *Cryptococcus neoformans*, Peptides 28 (2007) 1509–1513.
[9] R. Eckert, Road to clinical efficacy: challenges and novel strategies for antimicrobial peptide development, Future Microbiol. 6 (2011) 635–651.
[10] K. Matsuzaki, Control of cell selectivity of antimicrobial peptides, Biochim. Biophys. Acta 1788 (2009) 1687–1692.
[11] S.R. Dennison, J. Wallace, F. Harris, D.A. Phoenix, Amphiphilic alpha-helical antimicrobial peptides and their structure/function relationships, Protein Pept. Lett. 12 (2005) 31–39.
[12] V. Dhople, A. Krukemeyer, A. Ramamoorthy, The human beta-defensin-3, an antibacterial peptide with multiple biological functions, Biochim. Biophys. Acta 1758 (2006) 1499–1512.
[13] J. Ochieng, G. Chaudhuri, Cystatin superfamily, J. Health Care Poor Underserved 21 (2010) 51–70.
[14] M. Aschi, A. Bozzi, R. Di Bartolomeo, R. Petruzzelli, The role of disulfide bonds and N-terminus in the structural properties of hepcidins: insights from molecular dynamics simulations, Biopolymers 93 (2010) 917–926.
[15] B. Stec, Plant thionins-the structural perspective, Cell. Mol. Life Sci. 63 (2006) 1370–1385.
[16] W.F. Li, G.X. Ma, X.X. Zhou, Apidaecin-type peptides: biodiversity, structure–function relationships and mode of action, Peptides 27 (2006) 2350–2359.
[17] J.R. Luque-Ortega, W. Van't Hof, E.C.I. Veerman, J.M. Saugar, L. Rivas, Human antimicrobial peptide histatin 5 is a cell-penetrating peptide targeting mitochondrial ATP synthesis in *Leishmania*, FASEB J. 22 (2008) 1817–1828.
[18] B.J. Cuthbertson, Y. Yang, E. Bachère, E.E. Büllesbach, P.S. Gross, A. Aumelas, Solution structure of synthetic penaeidin-4 with structural and functional comparisons with penaeidin-3, J. Biol. Chem. 280 (2005) 16009–16018.
[19] Y.J. Gordon, E.G. Romanowski, A review of antimicrobial peptides and their therapeutic potential as anti-infective drugs, Curr. Eye Res. 30 (2005) 505–515.
[20] Y. Lan, Y. Ye, J. Kozlowska, J.K. Lam, A.F. Drake, A.J. Mason, Structural contributions to the intracellular targeting strategies of antimicrobial peptides, Biochim. Biophys. Acta 1798 (2010) 1934–1943.
[21] K.A. Markossian, A.A. Zamyatnin, B.I. Kurganov, Antibacterial proline-rich oligopeptides and their target proteins, Biochemistry (Mosc.) 69 (2004) 1082–1091.
[22] M. Scocchi, D. Romeo, M. Zanetti, Molecular cloning of Bac-7, a proline and arginine-rich antimicrobial peptide from bovine neutrophils, FEBS Lett. 26 (1994) 197–200.
[23] Y. Tokunaga, T. Niidome, T. Hatakeyama, H. Aoyagi, Antibacterial activity of bactenecin 5 fragments and their interaction with phospholipid membranes, J. Pept. Sci. 7 (2001) 297–304.
[24] M. Zanetti, Cathelicidins, multifunctional peptides of the innate immunity, J. Leukoc. Biol. 75 (2004) 39–48.
[25] P. Dolashka, V. Moshtanska, V. Borisova, A. Dolashki, S. Stevanovic, T. Dimanov, W. Voelter, Antimicrobial proline-rich peptides from the hemolymph of marine snail *Rapana venosa*, Peptides 32 (2011) 1477–1483.
[26] J.H. Cho, C.B. Park, Y.G. Yoon, S.C. Kim, Lumbricin I, a novel proline-rich antimicrobial peptide from the earthworm: purification, cDNA cloning and molecular characterization, Biochim. Biophys. Acta 1408 (1998) 67–76.
[27] M. Scocchi, A. Tossi, R. Gennaro, Proline-rich antimicrobial peptides: converging to a non-lytic mechanism of action, Cell. Mol. Life Sci. 68 (2011) 2317–2330.
[28] M. Gaczynska, P.A. Osmulski, Y. Gao, M.J. Post, M. Simons, Proline and arginine-rich peptides constitute a novel class of allosteric inhibitors of proteasome activity, Biochemistry 42 (2003) 8663–8670.
[29] J. Shi, C.C. Ross, L.T. Leto, F. Blecha, PR-39, a proline-rich antibacterial peptide that inhibits phagocyte NADPH oxidase activity by binding to Src homology 3 domains of p47 phox, Proc. Natl. Acad. Sci. U. S. A. 93 (1996) 6014–6018.
[30] Y.R. Chan, R.L. Gallo, PR-39, a syndecan-inducing antimicrobial peptide, binds and affects $p130^{Cas}$, J. Biol. Chem. 273 (1998) 28978–28985.
[31] T. Cabras, R. Longhi, F. Secundo, G. Nocca, S. Conti, L. Polonelli, C. Fanali, R. Inzitari, R. Petruzzelli, I. Messana, M. Castagnola, A. Vitali, Structural and functional characterization of the porcine proline-rich antifungal peptide SP-B isolated from salivary gland granules, J. Pept. Sci. 14 (2008) 251–260.
[32] C. Fanali, R. Inzitari, T. Cabras, A. Fiorita, E. Scarano, M. Patamia, R. Petruzzelli, A. Bennick, I. Messana, M. Castagnola, Mass spectrometry strategies applied to the characterization of proline-rich peptides from secretory parotid granules of pig (*Sus scrofa*), J. Sep. Sci. 31 (2008) 516–522.
[33] G.B. Fields, R.L. Noble, Solid phase peptide synthesis utilizing 9-fluorenylmethoxycarbonyl amino acids, Int. J. Pept. Protein Res. 35 (1990) 161–214.
[34] E. Atherton, R.C. Sheppard, in: S. Udenfriend, J. Meienhofer (Eds.), The fluorenylmethoxycarbonyl amino protecting group, The peptides, 9, Academic Press, San Diego, 1987, pp. 1–39.
[35] L. Whitmore, B.A. Wallace, Protein secondary structure analyses from circular dichroism spectroscopy: methods and reference databases, Biopolymers 89 (2008) 392–400.
[36] L. Polonelli, W. Magliani, S. Conti, L. Bracci, L. Lozzi, P. Neri, D. Adriani, F. de Bernardis, A. Cassone, Therapeutic activity of an engineered synthetic killer antiidiotypic antibody fragment against experimental mucosal and systemic candidiasis, Infect. Immun. 71 (2003) 6205–6212.
[37] E. Borenfreund, O. Borrero, In vitro cytotoxicity assays. Potential alternatives to the Draize ocular allergy test, Cell Biol. Toxicol. 1 (1984) 55–65.
[38] J.C. Wataha, R.G. Craig, C.T. Hanks, Precision of new methods for testing *in vitro* alloy cytotoxicity, Dent. Mater. 8 (1992) 65–70.
[39] I.A. Hashieh, A. Cosset, J.C. Franquin, J. Camps, In vitro cytotoxicity of one-step dentin bonding systems, J. Endod. 25 (1999) 89–92.
[40] S. Kolusheva, T. Shahal, R. Jelinek, Peptide-membrane interactions studied by a new phospholipid/polydiacetylene colorimetric vesicle assay, Biochemistry 39 (2000) 15851–15859.
[41] F. Lavialle, R.G. Adams, I.W. Levin, Infrared spectroscopic study of the secondary structure of melittin in water, 2-chloroethanol, and phospholipid bilayer dispersions, Biochemistry 21 (1982) 2305–2312.
[42] R. Gatti, G. Orlandini, J. Uggeri, S. Belletti, C. Galli, M. Raspanti, R. Scandroglio, S. Guizzardi, Analysis of living cells grown on different titanium surfaces by time-lapse confocal microscopy, Micron 39 (2008) 137–143.
[43] A.R. Viguera, J.R.L. Arrondo, A. Musacchio, M. Saraste, L. Serrano, Characterization of the interaction of natural proline-rich peptides with five different SH3 domains, Biochemistry 33 (1994) 10925–10933.
[44] T.P. Creamer, Left handed polyproline II helix formation is (very) locally driven, Proteins 33 (1998) 218–226.
[45] B.J. Stapley, T.P. Creamer, A survey of left-handed polyproline II helices, Protein Sci. 8 (1999) 587–595.
[46] C. Simon, I. Pianet, E.J. Dufourc, Synthesis and circular dichroism study of the human salivary proline-rich protein IB7, J. Pept. Sci. 9 (2003) 125–131.
[47] B. Bochicchio, A.M. Tamburro, Polyproline-II structure in proteins: identification by chiroptical spectroscopies, stability, and functions, Chirality 14 (2002) 782–792.
[48] A. Barth, The infrared absorption of amino acid side chains, Prog. Biophys. Mol. Biol. 74 (2000) 141–173.
[49] M. Moradi, V. Babin, C. Roland, T.A. Darden, C. Sagui, Conformations and free energy landscapes of polyproline peptides, Proc. Natl. Acad. Sci. U. S. A. 106 (2009) 20746–20751.
[50] B.J. Mayer, K. Saksela, SH3 domains, in: G. Cesareni, M. Gimona, M. Sudol, M. Yaffe (Eds.), Modular protein domains, Wiley-VCH, Weinheim, 2004, pp. 37–58.
[51] L. Otvos Jr., The short proline-rich antibacterial peptide family, Cell. Mol. Life Sci. 59 (2002) 1138–1150.

[52] M. Benincasa, M. Scocchi, E. Podda, B. Skerlavaj, L. Dolzani, R. Gennaro, Antimicrobial activity of Bac7 fragments against drug resistant clinical isolates, Peptides 25 (2004) 2055–2061.
[53] P.A. Raj, M. Edgerton, Functional domain and polyproline II conformation for candidicidal activity of bactenecin-5, FEBS Lett. 368 (1995) 526–530.
[54] H. Duclohier, How do channel- and pore-forming helical peptides interact with lipid membranes and how does this account for their antimicrobial activity? Mini Rev. Med. Chem. 23 (2002) 31–42.
[55] S. Pujals, E. Giralt, Proline-rich, amphipathic cell-penetrating peptides, Adv. Drug Deliv. Rev. 60 (2008) 473–484.